VIP Targeted PET Imaging

DOI: 10.1002/anie.201006579

Synthesis and In Vivo Imaging of a ^{18}F-Labeled PARP1 Inhibitor Using a Chemically Orthogonal Scavenger-Assisted High-Performance Method**

*Thomas Reiner, Edmund J. Keliher, Sarah Earley, Brett Marinelli, and Ralph Weissleder**

Poly-ADP-ribose-polymerases (PARPs) and breast cancer susceptibility proteins (BRCAs) are proteins that repair DNA breaks that occur during each cell cycle, and which must be repaired for a cell to survive. PARP repairs single-strand breaks and BRCA repairs double-strand breaks. In the absence of functional BRCA (e.g. when BRCA is mutated), PARP will repair both types of DNA breaks. Thus, PARP inhibitors (PARPis) are emerging as a useful therapeutic option (as a single agent or in combination with cytotoxic drugs), particularly for BRCA-negative tumors.[1] Several small-molecule PARP1is have been developed (e.g. olaparib/AZD2281, BSI101, AG014699, MK4827), and some of them are in clinical trials.[1–3] One problem in the assessment of therapeutic efficacy has been the inability to image PARP1 noninvasively at the whole-body level and to quantitate therapeutic inhibition. With this type of technology it would be possible to separate patients into appropriate treatment groups and to detect emerging resistance.[4] The design of PARP1 imaging agents—like that of most other intracellular imaging agents—is complex and time-consuming, and iterative approaches are often required to develop suitable compounds.

Given the emerging importance of positron emission tomography (PET) imaging in preclinical and clinical settings[5–9] and evidence that fluorescently labeled PARP1 inhibitors could be used for cellular imaging,[10] we became interested in developing ^{18}F-labeled probes for whole-body PARP1 imaging. Such radio-tracers could be particularly useful for measuring target inhibition of emerging therapeutic PARP1 inhibitors. Labeling native AZD2281 (**4**; Figure 1 D) at the 2-fluorobenzamide position has been challenging because of the fluorine's inaccessibility. In addition, modification of the piperazine moiety and subsequent nucleophilic fluorination is inefficient or results in decomposition of materials.[11] Furthermore, not all labeled high-affinity ligands identified in cell screens will exhibit ideal pharmacokinetics (blood half-life, tissue distribution, excretion) for PET imaging.

One way to identify useful imaging agents is to empirically test a series of different agents in vivo. This approach, however, places considerable demands on the labeling of each compound. First, fluorination must be optimized for every single compound and the desired products must be separated from the nonlabeled substrates so that the biological target is not inhibited by co-injection of the latter. Labeling and separation are usually performed using automated units enclosed by lead shields under time constraints because of the short half-life of ^{18}F (109.8 min). Given these lengthy sequential optimization procedures for each individual compound, it would be tremendously useful to develop more facile and straightforward platform technologies to advance the development of imaging agents through high-throughput synthesis and subsequent multiplexed in vivo testing. Herein we describe one such approach based on the combination of [4+2] inverse-electron-demand Diels–Alder cycloadditions and show its utility for the development of novel PARP1 PET imaging agents.

The [4+2] cycloaddition between *trans*-cyclooctene (TCO) and tetrazine (Tz) is a highly useful chemically orthogonal strategy.[10–14] The reaction is fast ($k > 6000\,\mathrm{M^{-1}s^{-1}}$) and highly selective; it does not require elevated temperatures or catalysts; the reaction conditions are biocompatible; the reaction tolerates blood, serum, and a wide variety of organic solvents; and activatable tetrazine dyes are readily available.[14–18] Despite the advantages and potentially broad utility of the [4+2] cycloaddition, there is currently little data on the biological behavior of dihydropyridazine and pyridazine linkers, for example, how these linkers affect the affinity of small molecules for their targets, if the conjugate modulates the pharmacokinetics in vivo, and whether this generic strategy could be used for in vivo PET imaging. Herein we describe a generic platform for parallel radiofluorination of small-molecule inhibitors and show how labeled reaction products can be rapidly isolated for subsequent in vivo testing before ^{18}F decays. We characterize TCO/Tz-generated ^{18}F-AZD2281 conjugates and describe biological and in vivo experiments. We show that one lead compound allows whole-body imaging of PARP1 and is useful for quantitating PARP1 inhibition in vivo. These results should pave the way for more extensive use of the [4+2] cycloaddition for the development of PET imaging agents.

[*] Dr. T. Reiner,[+] Dr. E. J. Keliher,[+] Dr. S. Earley, B. Marinelli, Prof. R. Weissleder
Center for Systems Biology, Massachusetts General Hospital
185 Cambridge Street, Boston, MA 02114 (USA)
Fax: (+1) 617-643-6133
E-mail: rweissleder@mgh.harvard.edu

[+] These authors contributed equally.

[**] We thank Dr. Ralph Mazitschek and Dr. Neal Devaraj for helpful discussions. This research was supported in part by the NIH (grants P50 CA86355 and RO1 EB-010011). T.R. received a stipend from the Deutschen Akademie der Wissenschaften Leopoldina (LPDS 2009-24).

Supporting information for this article is available on the WWW under http://dx.doi.org/10.1002/anie.201006579.

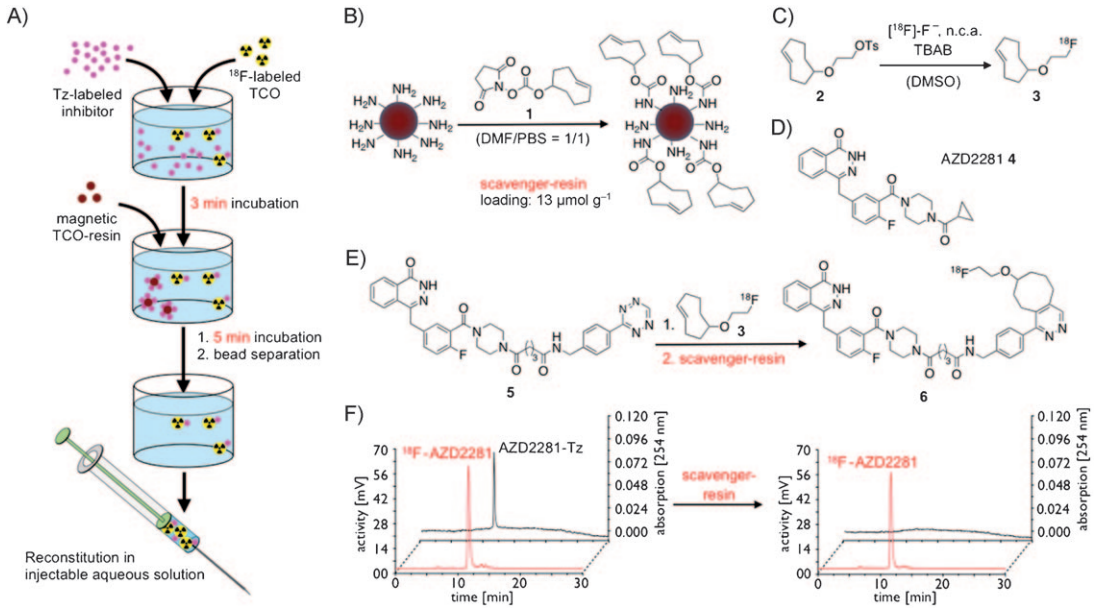

Figure 1. A) Schematic synthesis of ^{18}F-AZD2281 (**6**); ^{18}F-labeled TCO **3** and AZD2281-Tz (**5**) were combined and incubated for 3 min; magnetic TCO-scavenger resin was added, incubated for 5 min, and removed; purified ^{18}F-AZD2281 was reconstituted and brought into an injectable volume. B) Synthesis of the magnetic TCO-scavenger resin from amine-decorated beads and NHS-activated TCO **1**. C) Synthesis of ^{18}F-labeled TCO **3**. D) Structure of AZD2281 (**4**). E) Synthesis and structure of ^{18}F-AZD2281 (**6**; only one isomer shown). F) Radioactivity and absorption traces of the ^{18}F-AZD2281 reaction mixture before and after purification with the magnetic TCO-scavenger resin.

The designed radiolabeled AZD2281 derivatives were based on tetrazines that react with radiolabeled *trans*-cyclooctene derivatives and that are covalently attached at the piperazine unit of AZD2281. We previously showed that attachment of substituents to this position only minimally perturbs the ability of the resulting AZD2281 derivatives to inhibit PARP1 activity.[10,11] One problem during the synthesis of ^{18}F-radiolabeled compounds is that in most cases large amounts of precursors are used to efficiently react with small quantities of ^{18}F. The resulting mixtures are typically purified by HPLC to remove the excess starting material, which in most cases will compete with the radiolabeled probe for the targeted binding sites. To avoid lengthy HPLC purifications, we designed a *trans*-cyclooctene resin to "pull out" excess tetrazine-conjugated AZD2281 derivatives from the reaction mixture (Figure 1 A). The resin was prepared by reaction of commercially available magnetic amine-decorated beads in a solution of DMF/PBS with a 75 mM solution of NHS-activated *trans*-cyclooctene **1** (Figure 1 B; NHS: *N*-hydroxysuccinimide). The resulting TCO-decorated beads were determined to have a loading of 13 μmol g^{-1} using tetrazine-labeled Oregon Green-Tz;[16] the absorbance of the latter at 504 nm was used to measure the quantity of material pulled out of solution by the beads (see the Supporting Information for detailed descriptions).

Chemically orthogonal reactive radiolabeled ^{18}F-TCO **3** was synthesized by nucleophilic substitution of the tosylate of *trans*-cyclooctene **2** by ^{18}F$^-$ (n.c.a.) in the presence of tetrabutylammonium bicarbonate (TBAB, Figure 1 C).[11] AZD2281-Tz (**5**) was synthesized as recently described.[11] For ^{18}F-AZD2281 (**6**), **3** (1000 μCi), and **5** (130 nmol) were combined in H_2O/DMSO and stirred vigorously for 3 min. This results in quantitative conversion of ^{18}F-TCO **3**, yielding a mixture of ^{18}F-AZD2281 (**6**) and excess AZD2281-Tz (**5**; Figure 1 E). Subsequently, treatment of this solution for 5 min with the TCO-decorated scavenger resin (4 mol equiv of TCO) removed unreacted AZD2281-Tz with minimal loss (approximately 4 %) of radiolabeled compound **6**. Magnetic removal of the beads provided **6** in (92.1 ± 0.4) % dcRCY, which was then reconstituted in a medium suitable for animal injection (Figure 1 A). HPLC analysis of the reaction mixture before and after treatment with the TCO-decorated scavenger resin shows that the absorption peak resulting from AZD2281-Tz completely vanishes, whereas the activity peak resulting from ^{18}F-AZD2281 persists (Figure 1 F).

The IC_{50} value of ^{18}F-AZD2281 against PARP1 was determined to be (17.9 ± 1.1) nM in biochemical assays using the isolated enzyme (AZD2281 itself has an IC_{50} value of 5 nM).[11,19,20] This demonstrates PARP1 to be an ideal target for the rapid screening of ^{18}F-labeled inhibitors, as it can accommodate relatively large prosthetic groups that do not affect binding affinity. To determine the inhibitor's performance in cell-based in vitro assays, MDA-MB-436 and MDA-MB-231 cells were plated (5×10^5 cells per well) and incubated at 37 °C overnight. Subsequently, both cell lines were incubated with either 5 μCi of ^{18}F-AZD2281 or a mixture of 5 μCi of ^{18}F-AZD2281 and AZD2281 (final concentration AZD2281: 10 μM–0.01 mM). Cellular uptake of ^{18}F-AZD2281 was determined by quantification of the remaining activity after incubation and washing of the adherent cells. ^{18}F-AZD2281 was shown to be cell-permeable and its uptake inhibitable upon addition of excess non-radioactive AZD2281 (Figure 2). Uptake of ^{18}F-AZD2281 was lower for MDA-MB-231 cells than for MDA-MB-436

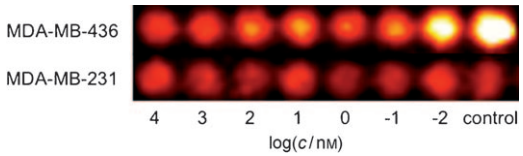

Figure 2. Competitive in vitro inhibition assays with ^{18}F-AZD2281. Cells containing either a high (MDA-MB-436) or a low amount of PARP1 (MDA-MB-231) were treated with 5 μCi of ^{18}F-AZD2281 in the presence of different concentrations of AZD2281 (10 μM–0.01 nM). After the cells were washed, cell-associated activity was determined by measurement of the γ-radiation. For the control measurement, no unlabeled AZD2281 was added.

cells, which correlates with protein expression of PARP1 in the respective cell lines (see the Supporting Information for details).

In subsequent in vivo experiments, 30 μCi of ^{18}F-AZD2281 were injected into Nu/Nu mice and imaged by PET/CT over a period of 2 h. Figure 3 A displays the distribution of the PET probe at 10, 30, and 50 min. The images clearly show initial localization of the probe to be mainly in liver, gall bladder, and intestines, consistent with hepatobiliary excretion. After 50 min (Figure 3 A), the majority of the probe had left the bloodstream ($t_{1/2} = 6$ min) and was excreted through the large intestines.

Tumor-bearing mice were obtained by injection of MDA-MB-436 cells (5×10^6 cells in matrigel) into the flanks of Nu/Nu mice, and the tumors were allowed to grow and vascularize for 7 days. Figure 3 B shows a three-dimensional reconstruction of a tumor-bearing mouse injected with 30 μCi of ^{18}F-AZD2281. Uptake in the tumors is clearly visible. Immediately after imaging, the mice were injected with 1 mg AZD2281 BID. Re-injection of 30 μCi of ^{18}F-AZD2281 confirmed inhibition of the probe's uptake into the tumors (Figure 3 B and C). Therefore, owing to the rapid decay rate of ^{18}F, each mouse serves as its own control on subsequent days of imaging, facilitating direct comparisons of SUVs.

In summary, we have showed a) that ^{18}F-AZD2281 accumulates in PARP1-overexpressing cancer cells (e.g. MDA-MB-436), b) the cellular accumulation can be inhibited by nonlabeled AZD2281, c) ^{18}F-AZD2281 accumulates in PARP1 mouse models of cancer in vivo, and d) PARP1 inhibition can be quantitated by PET imaging in vivo. The imaging agent was developed in relatively short time using the above described chemically orthogonal scavenger-assisted high-performance method. Scavenger beads for alternative conjugation methods could also be developed and applied in similar ways. However, we believe that the described method is particularly appealing for development of PET imaging agents because of the extremely fast kinetics of the tetrazine/*trans*-cyclooctene inverse-electron-demand Diels–Alder reaction at room temperature, its independence of catalysts, and high selectivity. The technology described can be readily expanded to other drugs, biomolecules, and molecular targets and should facilitate the development of PET imaging agents for drug testing.

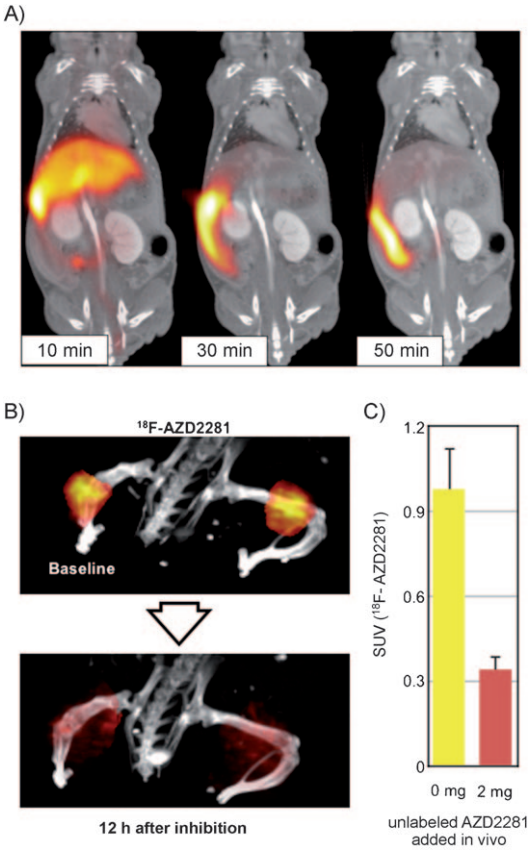

Figure 3. In vivo evaluation of ^{18}F-AZD2281. A) Combined PET/CT scans of a nontumor-bearing mouse injected with ^{18}F-AZD2281 recorded 10, 30, and 50 min after injection. B) Three-dimensional reconstruction of a tumor-bearing animal injected with ^{18}F-AZD2281 with and without pre-injection of AZD2281 (bladder segmented out for clarity). C) Quantification of uptake through the tumor in hind legs with and without intraperitoneal pre-injection of unlabeled AZD2281 SUV: standardized uptake value

Received: October 20, 2010
Published online: January 21, 2011

Keywords: cancer therapy · chemically orthogonal conjugation · in vivo imaging · positron emission tomography · scavenger resin

[1] M. Rouleau, A. Patel, M. J. Hendzel, S. H. Kaufmann, G. G. Poirier, *Nat. Rev. Cancer* **2010**, *10*, 293–301.
[2] K. Ratnam, J. A. Low, *Clin. Cancer Res.* **2007**, *13*, 1383–1388.
[3] E. A. Comen, M. Robson, *Oncology* **2010**, *24*, 55–62.
[4] R. Weissleder, M. J. Pittet, *Nature* **2008**, *452*, 580–589.
[5] N. Avril, C. A. Rosé, M. Schelling, J. Dose, W. Kuhn, S. Bense, W. Weber, S. Ziegler, H. Graeff, M. Schwaiger, *J. Clin. Oncol.* **2000**, *18*, 3495–3502.
[6] H. D. Burns et al., *Proc. Natl. Acad. Sci. USA* **2007**, *104*, 9800–9805.
[7] S. S. Gambhir, *Nat. Rev. Cancer* **2002**, *2*, 683–693.
[8] J. K. Willmann, N. van Bruggen, L. M. Dinkelborg, S. S. Gambhir, *Nat. Rev. Drug Discovery* **2008**, *7*, 591–607.
[9] M. T. Klimas, *Mol Imaging Biol.* **2002**, *4*, 311–337.
[10] T. Reiner, S. Earley, A. Turetsky, R. Weissleder, *ChemBioChem* **2010**, 11, 2374–2377.
[11] E. J. Keliher, T. Reiner, A. Turetsky, R. Weissleder, *ChemMedChem* **2010**, DOI: 10.1002/cmdc.201000426.

[12] P. V. Chang, J. A. Prescher, E. M. Sletten, J. M. Baskin, I. A. Miller, N. J. Agard, A. Lo, C. R. Bertozzi, *Proc. Natl. Acad. Sci. USA* **2010**, *107*, 1821 – 1826.
[13] M. L. Blackman, M. Royzen, J. M. Fox, *J. Am. Chem. Soc.* **2008**, *130*, 13518 – 13519.
[14] N. K. Devaraj, R. Upadhyay, J. B. Haun, S. A. Hilderbrand, R. Weissleder, *Angew. Chem.* **2009**, *121*, 7147 – 7150; *Angew. Chem. Int. Ed.* **2009**, *48*, 7013 – 7016.
[15] N. K. Devaraj, S. Hilderbrand, R. Upadhyay, R. Mazitschek, R. Weissleder, *Angew. Chem.* **2010**, *122*, 2931 – 2934; *Angew. Chem. Int. Ed.* **2010**, *49*, 2869 – 2872.
[16] N. K. Devaraj, E. J. Keliher, G. M. Thurber, M. Nahrendorf, R. Weissleder, *Bioconjugate Chem.* **2009**, *20*, 397 – 401.
[17] N. K. Devaraj, R. Weissleder, S. A. Hilderbrand, *Bioconjugate Chem.* **2008**, *19*, 2297 – 2299.
[18] J. B. Haun, N. K. Devaraj, S. A. Hilderbrand, H. Lee, R. Weissleder, *Nat. Nanotechnol.* **2010**, *5*, 660 – 665.
[19] D. V. Ferraris, *J. Med. Chem.* **2010**, *53*, 4561 – 4584.
[20] K. A. Menear, C. Adcock, R. Boulter, X.-l. Cockcroft, L. Copsey, A. Cranston, K. J. Dillon, J. Drzewiecki, S. Garman, S. Gomez, H. Javaid, F. Kerrigan, C. Knights, A. Lau, V. M. Loh, Jr., I. T. W. Matthews, S. Moore, M. J. O'Connor, G. C. M. Smith, N. M. B. Martin, *J. Med. Chem.* **2008**, *51*, 6581 – 6591.

